MOLECULAR AND CELLULAR BIOLOGY, Feb. 2009, p. 736–744 Vol. 29, No. 3
0270-7306/09/$08.00+0 doi:10.1128/MCB.01313-08

Loss of Mouse *Ikbkap*, a Subunit of Elongator, Leads to Transcriptional Deficits and Embryonic Lethality That Can Be Rescued by Human *IKBKAP*▽†

Yei-Tsung Chen, Matthew M. Hims, Ranjit S. Shetty, James Mull, Lijuan Liu, Maire Leyne, and Susan A. Slaugenhaupt*

Center for Human Genetic Research, Massachusetts General Hospital and Harvard Medical School, Boston, Massachusetts 02114

Received 18 August 2008/Returned for modification 8 September 2008/Accepted 8 November 2008

Familial dysautonomia (FD), a devastating hereditary sensory and autonomic neuropathy, results from an intronic mutation in the *IKBKAP* gene that disrupts normal mRNA splicing and leads to tissue-specific reduction of *IKBKAP* protein (IKAP) in the nervous system. To better understand the roles of IKAP in vivo, an *Ikbkap* knockout mouse model was created. Results from our study show that ablating *Ikbkap* leads to embryonic lethality, with no homozygous *Ikbkap* knockout (*Ikbkap*$^{-/-}$) embryos surviving beyond 12.5 days postcoitum. Morphological analyses of the *Ikbkap*$^{-/-}$ conceptus at different stages revealed abnormalities in both the visceral yolk sac and the embryo, including stunted extraembryonic blood vessel formation, delayed entry into midgastrulation, disoriented dorsal primitive neural alignment, and failure to establish the embryonic vascular system. Further, we demonstrate downregulation of several genes that are important for neurulation and vascular development in the *Ikbkap*$^{-/-}$ embryos and show that this correlates with a defect in transcriptional elongation-coupled histone acetylation. Finally, we show that the embryonic lethality resulting from *Ikbkap* ablation can be rescued by a human *IKBKAP* transgene. For the first time, we demonstrate that IKAP is crucial for both vascular and neural development during embryogenesis and that protein function is conserved between mouse and human.

IKBKAP (encoding IκB kinase-associated protein, also called Elongator protein 1) is the gene mutated in hereditary sensory and autonomic neuropathy type III, or familial dysautonomia (FD). All FD patients carry at least one copy of a splicing mutation in *IKBKAP*, which causes aberrant exon skipping and subsequent tissue-specific reduction of protein expression in FD patients (1, 41, 42). The *IKBKAP* gene is highly conserved across species, with the human and mouse proteins (IKAP and Ikap, respectively) sharing more than 80% amino acid homology (12). The *IKBKAP* protein, IKAP, was first reported to act as a scaffolding protein for the IκB kinase complex (11). Recent studies, however, have shown that IKAP does not play a role in NF-κB (nuclear factor κB) signaling, but rather, it is a subunit of the human Elongator complex, which is important for efficient transcriptional elongation (19, 28, 36).

FD (or Riley-Day syndrome) is one of the best known recessive hereditary neuropathies, with an extremely high carrier frequency in the Ashkenazi Jewish population, which ranges from 1 in 17 to 1 in 28 depending on the country of origin (29, 33, 42). Clinical characteristics of FD include diminished tear secretion, dysphagia, esophageal and gastric dysmotility, gastroesophageal reflux, spinal curvature, postural hypotension, blotching, excessive sweating, and decreased deep-tendon reflexes (2). Fatality in FD patients is high, and only half survive to 40 years of age. Clinical reports have shown that the failure of autonomic function is one of the major causes of death (21). To date, three FD-causing mutations have been identified in the *IKBKAP* gene: an intronic noncoding point mutation, IVS20+6T>C, and two missense mutations, R696P and P914L. All FD patients carry at least one copy of the noncoding point mutation in the *IKBKAP* gene, with over 99.5% homozygous for this mutation. The IVS20+6T>C mutation in intron 20 disrupts the splicing of *IKBKAP* and results in variable skipping of exon 20 in the *IKBKAP* transcript (1, 30, 41). Our studies have demonstrated that homozygous mutant cells derived from FD patients express both wild-type and mutant *IKBKAP* mRNA and are capable of synthesizing full-length functional IKAP protein (41). Thus, the *IKBKAP* mutation weakens but does not completely inactivate the 5′ splice site of exon 20. Indeed, this finding was further supported by the presence of both wild-type and mutant *IKBKAP* mRNAs in tissues from FD patients (17, 41). Interestingly, the relative amounts of wild-type and mutant *IKBKAP* transcripts vary between tissues. In particular, the central and peripheral nervous systems contain the lowest levels of wild-type *IKBKAP* mRNA and protein (13, 41), corresponding to the observed developmental absence and ongoing degeneration of unmyelinated sensory and autonomic neurons seen in FD (2, 38). Heterozygous carriers also show reduced IKAP expression; however, no phenotype is evident, suggesting that there is a tissue-specific minimum threshold of IKAP expression required for normal development and maintenance of the nervous system.

Although the correlation between the *IKBKAP* mutation and FD is well documented, precisely how a tissue-specific reduction of IKAP leads to the development of FD remains to

* Corresponding author. Mailing address: Center for Human Genetic Research, Massachusetts General Hospital, CPZN-5254, 185 Cambridge Street, Boston, MA 02114. Phone: (617) 643-3091. Fax: (617) 643-3202. E-mail: Slaugenhaupt@chgr.mgh.harvard.edu.

† Supplemental material for this article may be found at http://mcb.asm.org.

▽ Published ahead of print on 17 November 2008.

be elucidated. Recently, by using RNA interference technology in HeLa cells, it was shown that an 80% reduction of *IKBKAP* transcript leads to a loss of integrity of the Elongator complex, which subsequently diminishes the expression of several genes that are known to be essential for cell motility. A subset of these genes was also shown to be downregulated in fibroblast lines derived from FD patients. Further, Elongator complex reduction was demonstrated to directly interfere with histone H3 acetylation of a specific subset of genes (10). Since the development of the nervous system requires extensive migration of differentiated neuronal progenitors to their target destinations, these findings suggest that defective cellular motility could be one underlying cause of the developmental neuropathology of FD. IKAP was also implicated in myelination based on minor gene expression differences detected by microarray analyses of RNAs isolated from the frontal cortexes of two normal and two FD individuals (8); however, this putative role for IKAP has not yet been functionally confirmed. In addition to regulating the transcriptional machinery, IKAP has been proposed to play a role in exocytosis, activation of JNK signaling, and tRNA modification (24, 25, 39). As pointed out in a recent review of the many putative functions of IKAP/Elongator, considerable work remains to sort out the precise function of IKAP/Elongator (46).

To better understand the role of IKAP in vivo, we created a mouse with a targeted disruption of the *Ikbkap* gene (*Ikbkap*$^{-/-}$) (GeneID, 230233). We demonstrate that homozygous disruption of the mouse *Ikbkap* gene leads to embryonic lethality prior to midgestation, since no *Ikbkap*$^{-/-}$ embryos could be recovered after 12.5 days postcoitum (dpc). Further analyses of the *Ikbkap*$^{-/-}$ conceptus from 7.5 to 10.5 dpc revealed several abnormal configurations compared with *Ikbkap*$^{+/+}$ controls, including a dramatic reduction in overall size, disruption of the extraembryonic vascular networks, failure of germ layer inversion, and interruption of cephalic neural-tube closure. Further, the expression of several genes that have been shown to be essential for embryogenesis is downregulated in the *Ikbkap*$^{-/-}$ embryos due to defective elongation of the transcript, suggesting a crucial role for *Ikbkap* during development. The murine Ikap protein is 80% identical to human IKAP, and we show that the embryonic lethality of *Ikbkap* ablation can be rescued by a human *IKBKAP* transgene. By crossing the *Ikbkap* knockout mouse line with human transgenic lines, we confirmed IKAP functional conservation between human and mouse. Taken together, our studies show for the first time that Ikap is required for embryogenesis in mammals. Elucidating how IKAP functions during development is a crucial first step toward discovering how reduction of IKAP expression leads to neuronal loss in FD.

MATERIALS AND METHODS

Animals. The *Ikbkap* knockout mouse line was generated in collaboration with BayGenomics (currently known as the International Gene Trap Consortium [IGTC]) (35). In brief, chimeras with the *Ikbkap* knockout allele were derived from embryonic cell lines that contain a gene trap vector at intron 9 of the *Ikbkap* gene. The gene trap vectors used by the IGTC were inserted randomly into introns and contained a splice-acceptor sequence followed by a β-galactosidase and neomycin phosphotransferase II (β-geo) cassette. The resulting insertion created a fusion transcript containing the exons upstream of the insertion joined to the β-geo cassette. The identity of the trapped/disrupted gene could easily be determined by 5′ rapid amplification of cDNA ends, followed by sequencing. Cell line BGB184 produced a transcript containing *Ikbkap* exons 1 to 9 and the β-geo cassette, and we later confirmed that the vector was inserted into intron 9. Mice with the C57BL/6J background used in this study were generated by serial backcrossing. The *Ikbkap*$^{+/+}$ and *Ikbkap*$^{-/-}$ embryos for this study were produced from heterozygous breeding pairs. The day of vaginal-plug discovery was designated 0.5 dpc. The transgenic mouse lines that carry human *IKBKAP* transgenes were generated as previously reported (23). The mice used for this study were housed in the animal facility of Massachusetts General Hospital (Boston, MA), provided with constant access to a standard diet of food and water, and maintained on a 12-hour light/dark cycle, and all experimental protocols were approved by the Subcommittee on Research Animal Care at the Massachusetts General Hospital.

Genotyping. The genotypes of animals and embryos were determined by PCR analysis of genomic DNA from tail slips and from embryos and/or visceral yolk sacs, respectively. The primer sets used were as follows: for determining the wild-type *Ikbkap* allele, 5′-ACCCTCAGGCAGTTTGATTG-3′ and 5′-CATGG CTCCATAAAACAAACAC-3′; for determining the knockout allele, 5′ACCC TCAGGCAGTTTGATTG-3′ and 5′-GGCTACCGGCTAAAACTTGA-3′; and for determining the human wild-type *IKBKAP* transgenes, TgProbe1F (5′-GCC ATTGTACTGTTTGCGACT-3′) and TgProbe1R (5′-TGAGTGTCACGATTC TTTCTGC-3′).

Morphological analysis of embryos. Photographs of visceral yolk sacs and embryos at different stages were taken with a digital camera (Diagnostic Instruments) mounted on an Olympus dissection microscope. SPOT software (Diagnostic Instruments) was used for image processing.

X-Gal staining of embryos. Embryos at different stages were dissected in cold phosphate-buffered saline (PBS) and fixed with 4% paraformaldehyde overnight. The embryos were then rinsed with PBS three times for 10 min each time and incubated with 1 mM 5-bromo-4-chloro-3-indolyl-β-D-galactoside (X-Gal) (Molecular Probes) in PBS at 37°C for 16 to 24 h. The embryos were rinsed with PBS and fixed in 4% paraformaldehyde before being imaged.

RT-PCR. Total RNA from visceral yolk sacs and whole embryos was extracted by using TRI Reagent (Molecular Research Center) according to the manufacturer's protocol. Reverse transcription (RT) was then performed using 1 μg total RNA, oligo(dT) primer, and Superscript III reverse transcriptase (Invitrogen) according to the manufacturer's protocol. For gene expression assessment, semiquantitative PCR was performed with the cDNA equivalent of 100 ng of starting RNA in a 30-μl reaction mixture, with the use of *Taq* polymerase (Roche) with target-specific primer pairs that were custom designed by OligoPerfect Designer (Invitrogen). For the primer sequences for RT-PCR analysis, see the supplemental material. Thirty-two amplification cycles (94°C for 30 s, 60°C for 35 s, and 72°C for 30 s) were then performed. The PCR products were separated on 1.5% agarose gels, stained with ethidium bromide, and visualized with UV light using the Alphaimager 2200 system (Alpha Innotech). Relative band intensities were determined by evaluating the integrated density values as determined by the Alphaimager 2000 software.

Acetyl-histone H3 ChIP assay. The immunocomplex containing chromatin fragments/anti-acetyl-histone H3 antibody/protein A/G agarose was extracted using an acetyl-histone H3 chromatin immunoprecipitation (ChIP) assay kit (Millipore) according to the manufacturer's protocol. In brief, formaldehyde-treated embryos were washed with PBS containing protease inhibitors (1 mM phenylmethylsulfonyl fluoride, 1 mg/ml aprotinin, and 1 mg/ml pepstatin A) and centrifuged at 4°C. The pellets were suspended in sodium dodecyl sulfate lysis buffer and incubated for 10 min, followed by sonication at 30% amplitude with a Microson XL2000 Ultrasonic cell disruptor (Misonix). The sonicated samples were then centrifuged, and the supernatant containing chromatin fragments was diluted with ChIP dilution buffer. The chromatin-containing dilutions were precleared with salmon sperm DNA/protein A agarose 50% slurry before overnight incubation with anti-acetyl-histone H3 antibody. The next day, samples were incubated with salmon sperm DNA–protein A-agarose 50% slurry at 4°C for 1 h. Finally, the protein A-agarose/antibody/histone complex was recovered by centrifugation and sequentially washed with low-salt, high-salt, LiCl, and Tris-EDTA buffers. For controls, an aliquot of the cross-linked/sonicated chromatin fraction was treated as described above without adding antibody, and the first supernatant, after being precleared with salmon sperm DNA–protein A-agarose 50% slurry, was saved as an input control. For PCR analysis, the histone-DNA complex was first eluted from the antibody, and the DNA fragment was released from the histone-DNA complex by adding NaCl and incubated for 4 h at 65°C. The DNA was then purified with a PCR purification kit (Qiagen) and analyzed by PCR with appropriate primer pairs corresponding to the coding regions of the testing genes. For the primer sequences, see the supplemental material. The PCR products were size fractionated by 1.5% agarose gel electrophoresis,

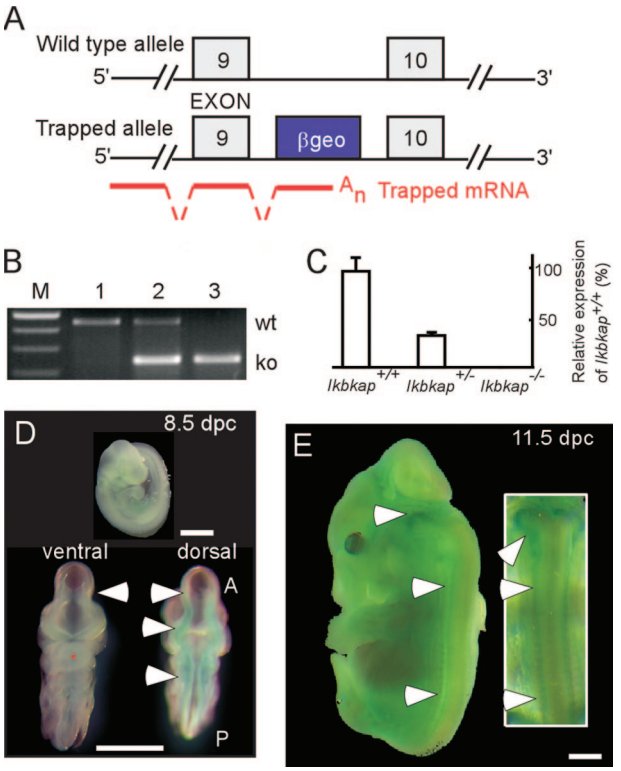

FIG. 1. Gene targeting strategy and *Ikbkap* expression. (A) Schematic of the wild-type and knockout *Ikbkap* alleles. The blue cassette (β-geo) represents the vector containing β-galactosidase, neomycin phosphotransferase II, and stop codons that is inserted into intron 9. The insertion creates a fusion transcript containing the exons upstream of the insertion joined to the β-geo marker, as illustrated by the red lines. (B) PCR genotyping results of genomic DNA from embryonic day 9.5 samples. Lanes 1, 2, and 3 represent the wild-type ($Ikbkap^{+/+}$), heterozygous ($Ikbkap^{+/-}$), and homozygous ($Ikbkap^{-/-}$) genotypes, respectively. wt, wild-type fragment (454 bp); ko, knockout fragment (244 bp). (C) The relative amounts of *Ikbkap* transcripts expressed in embryos with different genotypes at 8.5 dpc as demonstrated by quantitative RT-PCR. The error bars indicate standard deviations. (D and E) X-Gal staining of whole-mount $Ikbkap^{+/-}$ embryos at 8.5 and 11.5 dpc, respectively. The arrowheads in panel D point to the ventral and dorsal neural tubes; note that the primitive hindbrain region shows higher positive reactivity. The arrowheads in panel E point to the hindbrain and dorsal ganglia. A, anterior; P, posterior. Scale bars, 1 mm.

stained with ethidium bromide, and visualized with UV light using the Alphaimager 2200 system (Alpha Innotech).

Western blots. Protein from brains was extracted using RIPA buffer (Boston BioProducts). An equivalent amount of protein (30 μg) was run on a 10% Bis-Tris gel (Invitrogen) and then transferred onto a Hybond-N^+ membrane (Amersham) using XCell SureLock Mini-Cell and XCell II Blot Module kits, respectively (Invitrogen), according to the manufacturer's protocol. Antibodies against the carboxyl terminus of human IKAP (1:3,000) (41), β-tubulin (1:3,000) (Santa Cruz Biotech), and rabbit/mouse immunoglobulin G-horseradish peroxidase conjugate secondary antibody (1:2,000) (Santa Cruz Biotech) were applied subsequently and visualized using the enhanced-chemiluminescence system (GE Healthcare UK, Ltd.) on X-ray film (Kodak).

RESULTS

Generation of an *Ikbkap* knockout mouse line. The *Ikbkap* knockout mouse line was generated utilizing gene trap technology in collaboration with the IGTC (35). This strategy has been widely used for functional analysis of mammalian genes (43). The gene trap vectors contain a splice-acceptor sequence, followed by the β-geo reporter gene and selection cassettes (a fusion of β-galactosidase and neomycin phosphotransferase II), which are randomly targeted to the 5′ ends of introns. The resulting inserted mutation creates a fusion transcript containing the exons upstream of the insertion joined to the β-geo marker. As a result, the identity of the trapped/disrupted gene can be determined by 5′ rapid amplification of cDNA ends followed by sequencing. Not only does successful gene trap insertion disrupt expression of the gene of interest, but the reporter cassette also provides a tag for characterizing the pattern of expression of the target gene. Chimeras that bear an *Ikbkap* knockout allele were derived from embryonic cell lines that contained a gene trap vector at intron 9 of the *Ikbkap* gene (Fig. 1A). The genotypes of specimens were determined by amplification of genomic DNA using wild-type and knockout primer sets (Fig. 1B). Mice heterozygous for the mouse *Ikbkap* knockout allele are fertile and phenotypically normal and show approximately 60% reduction in mouse *Ikbkap* expression when evaluated by quantitative RT-PCR (Fig. 1C). The mice used in this study were on a C57BL/6J background and were created by serial backcrossing for 10 generations; concurrently, heterozygote matings were used to generate offspring ($Ikbkap^{+/+}$, $Ikbkap^{+/-}$, and $Ikbkap^{-/-}$). In addition, X-Gal staining was employed to visualize the expression of *Ikbkap*, as well as to confirm successful trap insertion in heterozygous embryos during development. At 8.5 and 11.5 dpc, positive signal could be observed from the entire embryo; however, intensities differed across tissues, with particularly high levels in the mid- and hindbrain walls, as well as the otic vesicle and dorsal ganglia (Fig. 1D and E). This IKAP expression pattern is similar to that reported in rats (34).

Ablation of *Ikbkap* results in embryonic lethality in mice. Heterozygous matings ($Ikbkap^{+/-} \times Ikbkap^{+/-}$) generated 74 $Ikbkap^{+/-}$ and 42 $Ikbkap^{+/+}$ mice, while no $Ikbkap^{-/-}$ animals were born, statistically demonstrating that knocking out *Ikbkap* results in embryonic lethality ($P < 0.005$). To pinpoint the time of embryonic death, timed matings were performed using 25 dams. Pregnant mice were sacrificed at time points ranging from 6.5 to 12.5 dpc, and 230 embryos were isolated. By performing PCR of genomic DNA isolated from either the embryo or yolk sac, the genotype of each embryo was determined. At 7.5 to 12.5 dpc, 59 $Ikbkap^{+/+}$, 121 $Ikbkap^{+/-}$, and 50 $Ikbkap^{-/-}$ embryos were obtained, values that are consistent with Mendelian segregation (Table 1). No embryos were re-

TABLE 1. Genotype ratios of yolk sacs and neonates produced by heterozygous pairings

Time[a]	No. (%) of animals			Total
	$Ikbkap^{+/+}$	$Ikbkap^{+/-}$	$Ikbkap^{-/-}$	
7.5–10.5 dpc	50 (26)	99 (52)	43 (22)	192
11.2–12.5 dpc	9 (24)	22 (58)	7 (18)	38
14.5–16.5 dpc	18 (33)	36 (67)	0 (0)	54
P0	42 (29)	74 (71)	0 (0)	116

[a] The time of conception is estimated to be 0.5 day prior to the observation of a vaginal plug. P0, postnatal day zero.

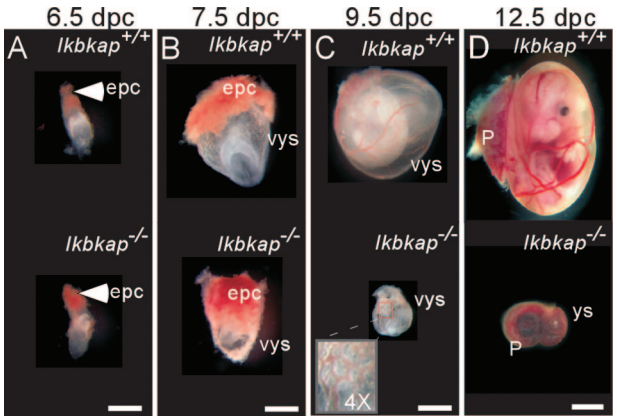

FIG. 2. Appearance of *Ikbkap*$^{+/+}$ and *Ikbkap*$^{-/-}$ extraembryonic components at different stages. Shown is the morphology of the *Ikbkap*$^{+/+}$ and *Ikbkap*$^{-/-}$ conceptus at 6.5 to 12.5 dpc under a dissection microscope. (A) At 6.5 dpc, no gross abnormalities are found in the *Ikbkap*$^{-/-}$ conceptus compared to a wild-type control. epc, ectoplacental cone. (B) At 7.5 dpc, the *Ikbkap*$^{-/-}$ epc and visceral yolk sac (vys), as well as the embryo inside, are smaller than those found in *Ikbkap*$^{+/+}$ controls. Note that at this stage the blood islands are readily observable in the *Ikbkap*$^{+/+}$ vys; however, no corresponding architectures are found in the *Ikbkap*$^{-/-}$ vys. (C) At 9.5 dpc, the *Ikbkap*$^{-/-}$ vys, as well as the embryo inside, are smaller than those found in the *Ikbkap*$^{+/+}$ control. At this stage, the blood vessels can easily be identified in the *Ikbkap*$^{+/+}$ vys; however, in the *Ikbkap*$^{-/-}$ vys, only the primary capillary plexus is observed (inset). (D) At 12.5 dpc, the placenta can be found in both genotypes; in contrast, no embryo can be seen inside the *Ikbkap*$^{-/-}$ vys. P, placenta. Scale bars, 0.5 mm (A and B), 1 mm (C), and 2.5 mm (D).

covered inside the *Ikbkap*$^{-/-}$ yolk sacs at 12.5 dpc, suggesting that the degeneration of embryos occurs prior to this stage.

Vascular abnormalities in the *Ikbkap*$^{-/-}$ extraembryonic components. Morphologically, at 6.5 dpc, the *Ikbkap*$^{+/+}$ and *Ikbkap*$^{-/-}$ concepti were comparable in size (Fig. 2A). However, by 7.5 and 9.5 dpc, the extraembryonic components were clearly smaller in the *Ikbkap*$^{-/-}$ conceptus (Fig. 2B and C). Further, at 7.5 dpc, while blood islands formed in the *Ikbkap*$^{+/+}$ visceral yolk sac, corresponding structures were not observed in the *Ikbkap*$^{-/-}$ conceptus (Fig. 2B). At 9.5 dpc, the extraembryonic vessels were established in the *Ikbkap*$^{+/+}$ visceral yolk sac; however, only the primary capillary plexus was observed in the *Ikbkap*$^{-/-}$ visceral yolk sac (Fig. 2C, inset). By 12.5 dpc, the *Ikbkap*$^{-/-}$ embryo had degenerated and was no longer visible in the yolk sac, leaving only brown aggregates of debris. Although the placenta was present in the *Ikbkap*$^{-/-}$ conceptus at this stage, it was dramatically reduced in size (Fig. 2D).

Disturbed vascular development in the *Ikbkap*$^{-/-}$ visceral yolk sac suggests that vasculogenesis and angiogenesis might be compromised. Since IKAP is required for efficient transcription of a vast number of genes, many of which have yet to be identified, we examined the expression of several genes known to be vital for the development of extraembryonic blood vessels (6, 9, 14, 16, 27, 40, 45, 47). Studies of *Tgfb1*, *Vegfa*, *Gata6*, and *Smad2* knockout mouse models have shown that ablating each of these genes results in stunted extraembryonic blood vessel formation, which subsequently leads to embryonic lethality. In addition, we evaluated *Flt1*, the receptor for *Vegfa*; *Hnf4a*, a target gene of *Gata6*; and *Tie1* and *Tie2* and their ligands *Angpt1* and *Angpt2*, which have been shown to be independent from *TGFb1* or *VEGF* signaling for the development and integrity of extraembryonic vascular networks. RNA was isolated from *Ikbkap*$^{+/+}$ and *Ikbkap*$^{-/-}$ visceral yolk sacs, and gene expression was evaluated by RT-PCR. Interestingly, with the exception of *Hnf4a*, we did not see downregulation of any of these genes in the *Ikbkap*$^{-/-}$ visceral yolk sac. In fact, the expression of *Tgfb1*, *Flt1*, *Tie1*, and *Tie2* was clearly elevated in the *Ikbkap*$^{-/-}$ yolk sac, which may be a compensatory response (Fig. 3). Given the robust expression of *Ikbkap* in the wild-type visceral yolk sac at this stage, these results suggest that the observed failure of yolk sac vascular development is not directly due to inefficient transcription of the genes tested.

Abnormal architecture of *Ikbkap*$^{-/-}$ embryos during development. At 7.5 to 8.5 dpc, wild-type embryos underwent gastrulation, as indicated by the presence of the allantois, the definitive node, head folds, and axial rotation. However, growth of *Ikbkap*$^{-/-}$ embryos appeared to be arrested at the late egg cylinder stage, and no distinct stage-related architectures were present (Fig. 4A and B). At 9.5 and 10 dpc, several distinguishing structural characteristics, such as the primitive brain, spinal cord, cardiac contraction, branchial arch, and limb buds, were observed in the *Ikbkap*$^{+/+}$ embryos; in contrast, the *Ikbkap*$^{-/-}$ embryos lacked these developmental features, exhibiting only a primitive heart, cephalic neural folds, and allantois, and growth appeared to be arrested at midgastrulation (Fig. 4C and D), a stage that was comparable to the *Ikbkap*$^{+/+}$ controls at 7.5 dpc (Fig. 4A). In addition, in the *Ikbkap*$^{-/-}$ embryos, although a heart-like vascular structure was formed at 9.5 dpc, no visible primitive nucleated red blood cells were observed compared to those in the *Ikbkap*$^{+/+}$ embryos at 10 dpc (Fig. 4C and D). At 10.5 dpc, brain structures, branchial arches, and limb buds were visible in the *Ikbkap*$^{+/+}$ embryos but absent in the *Ikbkap*$^{-/-}$ embryos (Fig. 5A and B). At 10.5 dpc, morphological transformation had progressed in the *Ikbkap*$^{-/-}$ embryos, as the cephalic neural folds were found to be closed and there was evidence of rotation (Fig. 5B). In addition, mid- and hindbrain wall-like structures were visible but were aligned irregularly on the dorsal side of the *Ikbkap*$^{-/-}$ embryos (Fig. 5B, inset). After 10.5 dpc, the *Ikbkap*$^{-/-}$ embryos showed no further development, as the 11.5-dpc embryos isolated appeared similar in structure. As described above, all concepti isolated at 12.5 dpc had embryo degeneration.

Transcriptional deficits in *Ikbkap*$^{-/-}$ embryos. As in the visceral yolk sac, no advanced vascular network was observed in the *Ikbkap*$^{-/-}$ embryos. Thus, the expression levels of a subset of the genes that are important for vascular development were analyzed in the embryos. Since expression was evaluated in individual embryos, the amount of RNA was very limited, and therefore, we chose *Vegfa*, *Flt1*, *Tie2*, and *Smad2* for analysis. Interestingly, RT-PCR showed dramatic downregulation of *Vegfa*, *Flt1*, and *Tie 2* in the *Ikbkap*$^{-/-}$ embryos, while the expression of *Smad2* was similar to that seen in normal embryos (Fig. 6). Given that the *Ikbkap*$^{-/-}$ embryos die during gastrulation, we also examined expression of *Bmp4*, *Rhoa*, and *Ctnnb1*, genes that show defects in neurulation in knockout mouse models (5, 18, 48, 49). These genes also show dramatic downregulation compared to expression in wild-type

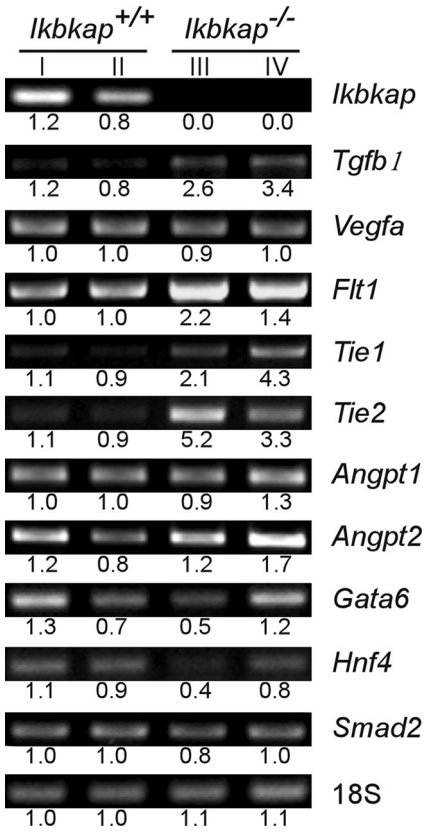

FIG. 3. Gene expression patterns of the *Ikbkap*$^{+/+}$ and *Ikbkap*$^{-/-}$ visceral yolk sac at 8.5 dpc. Shown is semiquantitative RT-PCR analysis of marker genes for vasculogenesis and angiogenesis at 8.5 dpc in the *Ikbkap*$^{+/+}$ and *Ikbkap*$^{-/-}$ visceral yolk sacs. The values represent the integrated density values of the bands relative to the average of the *Ikbkap*$^{+/+}$ expression. The names of the genes examined and the genotypes of samples are indicated. The samples in lane I and lane III, as well as lane II and lane IV, were harvested from littermates.

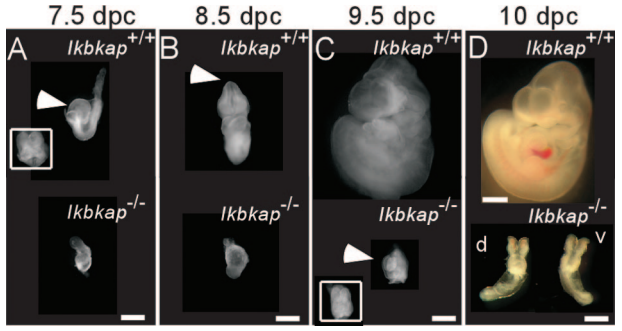

FIG. 4. Appearance of *Ikbkap*$^{+/+}$ and *Ikbkap*$^{-/-}$ embryos at different embryonic stages. Shown are morphological phenotypes of the *Ikbkap*$^{+/+}$ and *Ikbkap*$^{-/-}$ embryos from 7.5 to 10 dpc. At 7.5 dpc, the *Ikbkap*$^{+/+}$ embryo undergoes gastrulation and formation of primitive organized structures, such as allantois and head folds (A, inset); however, the *Ikbkap*$^{-/-}$ embryos appeared to be arrested at the late primitive streak stage, and this feature persisted to 8.5 dpc in the *Ikbkap*$^{-/-}$ embryo (B). At 8.5 and 9.5 dpc, closure of the anterior neural tube (arrowheads in panels B and C) and body rotation could be observed in wild-type embryos (B and C); in contrast, the *Ikbkap*$^{-/-}$ embryos lacked these developmental features (B and C). At 9.5 and 10 dpc, the characteristics of the midgastrulation stage, such as allantois, primitive heart, and head fold (C, inset, and D), could be found in the *Ikbkap*$^{-/-}$ embryo; however, no blood vessels were observed compared with the *Ikbkap*$^{+/+}$ control (D). Scale bars, 0.5 mm; in panel D, the scale bar adjacent to the *Ikbkap*$^{+/+}$ embryo is 1 mm.

embryos (Fig. 6). To determine the extent of the transcriptional downregulation in *Ikbkap*$^{-/-}$ embryos, we then tested the expression of genes, such as *Gelsolin*, *Beclin*, *P57*, and *Mmp2*, that were previously shown to be downregulated in response to IKAP reduction via small interfering RNA in various in vitro models (10). Interestingly, we did not see downregulation of these genes in *Ikbkap*$^{-/-}$ embryos at 8.5 dpc. Likewise, expression levels of *Elp2* (*StIP1* and *Statip1*) and *Elp3* (*KAT9*), which together with IKAP form the Elongator complex, were similar in *Ikbkap*$^{+/+}$ and *Ikbkap*$^{-/-}$ embryos. Elongator has histone acetyltransferase activity via its Elp3 subunit, and histone acetylation plays a major role in transcriptional regulation by altering the chromatin structure and therefore the accessibility of polymerases to the DNA (19, 20, 44). Indeed, in a previous study, transcriptional impairment in FD patient fibroblasts was shown to be correlated with histone H3 hypoacetylation in the transcribed regions of genes (10). To examine whether a deficiency in transcriptional elongation and histone acetylation might contribute to the observed downregulation of gene expression in *Ikbkap*$^{-/-}$ embryos, the acetylation of histone H3 in various transcribed regions of the genes was assessed using ChIP. As illustrated by PCR, the acetylation patterns near the transcriptional start sites of *Ctnnb1* (exon 2), *Bmp4* (exon 1), *Vegfa* (exon 1), and *Smad2* (exon 1) were compatible between *Ikbkap*$^{+/+}$ and *Ikbkap*$^{-/-}$ samples, indicating that histone H3 acetylation at promoters and during early transcript elongation was not perturbed. However, acetylation in the downstream coding regions of

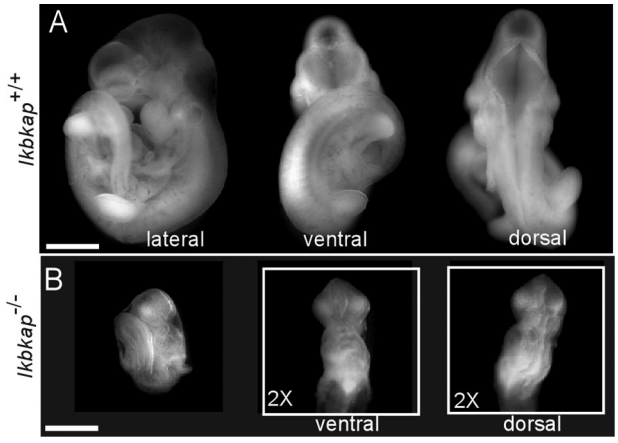

FIG. 5. Appearance of *Ikbkap*$^{+/+}$ and *Ikbkap*$^{-/-}$ embryos at 10.5 dpc. Shown is a morphological analysis of the *Ikbkap*$^{+/+}$ and *Ikbkap*$^{-/-}$ embryos at 10.5 dpc. (A) At this stage, in the *Ikbkap*$^{+/+}$ embryo, structures of the forebrain and hindbrain can be identified from ventral and dorsal aspects of the embryo, and the forelimb and hindlimb buds can be seen. (B) In contrast, at 10.5 dpc, incomplete turning is observed in the *Ikbkap*$^{-/-}$ embryo. No corresponding primitive brain structures or limb buds can be located; however, the anterior neural tube is closed from the ventral view, and the unsmooth zipper-like posterior neural tube can be found. Scale bars, 1 mm (A) and 0.5 mm (B).

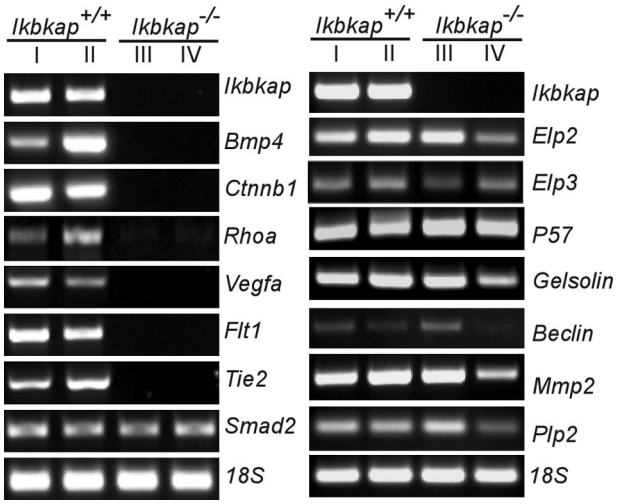

FIG. 6. Gene expression patterns of the *Ikbkap*$^{+/+}$ and *Ikbkap*$^{-/-}$ embryos at 8.5 dpc. Shown is RT-PCR analysis of genes using RNA isolated from *Ikbkap*$^{+/+}$ and *Ikbkap*$^{-/-}$ embryos. The names of the genes examined and genotypes of samples are indicated. Note that the samples in lane I and lane III, as well as lane II and lane IV, were harvested from littermates.

Ctnnb1, *Bmp4*, and *Vegfa* (exons 8, 2, and 3, respectively) was significantly reduced in *Ikbkap*$^{-/-}$ embryos (Fig. 7). These data suggest that, at least for this subset of genes, developmental loss of *Ikap* leads to defective histone acetylation during transcript elongation.

Rescue of *Ikbkap*$^{-/-}$ embryonic lethality by human IKAP. The embryonic lethality of the *Ikbkap*$^{-/-}$ mice stands in sharp contrast to the clinically observed survival of FD patients beyond the adolescent years. However, this result was anticipated, since the expression of IKAP is completely abolished in the mouse model while variable levels of normal IKAP are produced in FD patients, with marked reduction in the central and peripheral nervous system (13, 41). We postulate that there is a tissue-specific minimum IKAP level that is required for normal development. This hypothesis is supported by the fact that all FD patients carry at least one copy of the IVS20+6T>C splice mutation, which leads to the observed tissue-specific splicing differences. Further, no extremely deleterious mutations have been identified in the *IKBKAP* gene, as the two other known mutations lead to missense changes in the protein. Recently, we described the creation of transgenic mouse lines that carry the normal human *IKBKAP* gene and the FD IVS20+6T>C mutation. All of these lines are phenotypically normal, and the IVS20+6T>C transgenics missplice *IKBKAP* in a tissue-specific manner that mimics what is seen in FD patients (23). To test whether embryonic lethality caused by ablation of mouse *Ikbkap* could be rescued by human IKAP, we crossed two transgenic lines, one carrying the normal *IKBKAP* gene and one with the IVS20+6T>C mutation, with *Ikbkap*$^{+/-}$ mice in order to introduce the human transgenes into the *Ikbkap* knockout mouse line. The *Ikbkap*$^{+/-}$ mice that carried the human *IKBKAP* transgenes were viable, and fertility was normal with no obvious abnormalities (data not shown). Subsequent pairing of these lines with heterozygous *Ikbkap* knockout mice yielded animals that carried the human *IKBKAP* transgenes on a homozygous *Ikbkap* knockout background. The normal human *IKBKAP* transgene completely rescued embryonic lethality (Fig. 8A and B). In addition, by using an antibody that recognized only human IKAP, we demonstrated exclusive expression of human wild-type IKAP in the *Ikbkap*$^{-/-}$ knockout mice (Fig. 8C). These mice are phenotypically normal without any obvious abnormalities. The FD transgene did not rescue embryonic lethality in the *Ikbkap*$^{-/-}$ mice, likely due to the very low level of normal IKAP expression (Fig. 8C). This result indicates that the lethality of *Ikbkap* ablation in mice can be overcome by the presence of the human *IKBKAP* gene. More importantly, it confirms the functional conservation of IKAP between human and mouse during development.

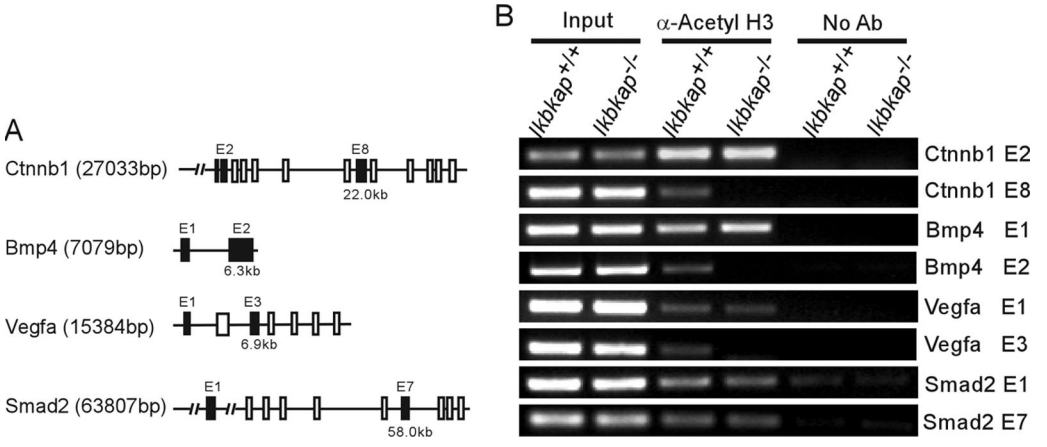

FIG. 7. Transcriptional analysis of *Ctnnb1*, *Bmp4*, *Vegfa*, and *Smad2* in *Ikbkap*$^{+/+}$ and *Ikbkap*$^{-/-}$ embryos. (A) Schematic representation of the genes investigated by ChIP assay. Exons are depicted by boxes; the closed boxes indicate the localization of the amplicons. The numbers (kb) indicate the positions of these amplicons relative to the 5′ sites of genes. (B) The acetylation status of histone H3 in the transcribed regions of *Ctnnb1*, *Bmp4*, *Vegfa*, and *Smad2* was estimated using an acetyl-histone H3 ChIP assay. Note that *Ctnnb1* exon 8, *Bmp4* exon 2, and *Vegfa* exon 3 were not pulled down with anti-acetyl-histone H3 antibody in *Ikbkap*$^{-/-}$ embryos. The genes tested, the genotypes, and the locations (E, exon) of amplicons are indicated. α-Acetyl H3, anti-acetyl-histone H3 antibody; No Ab, no antibody control.

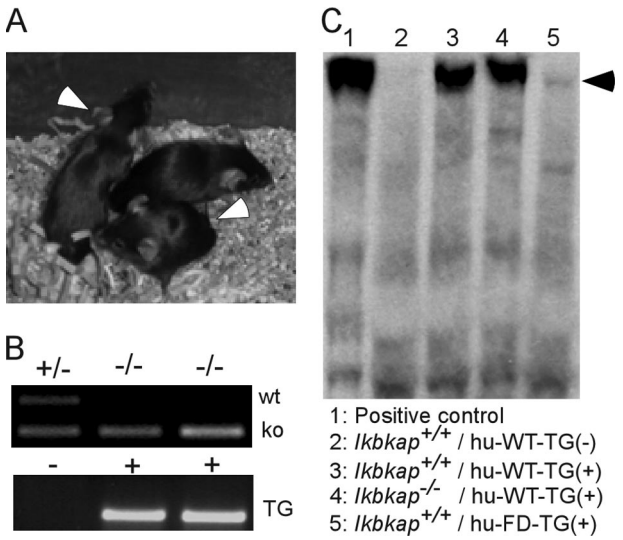

FIG. 8. Appearance of *Ikbkap*$^{-/-}$ mice with a human wild-type *IKBKAP* transgene. (A) The arrowheads point to *Ikbkap* null mice with the human wild-type *IKBKAP* transgene. No significant phenotypic differences were observed compared to heterozygous littermates. (B) PCR genotyping results of genomic DNA from tail snips with dedicated primers. Lane 1 (from left), *Ikbkap*$^{+/-}$genotype; lanes 2 and 3, *Ikbkap1*$^{-/-}$ genotype. The mice represented by lanes 2 and 3 were positive for carrying the human transgene. wt, wild-type fragment; ko, knockout fragment; TG, human *IKBKAP* transgene. (C) Western blot result using the human-specific IKAP antibody to confirm the presence of the human *IKBKAP* protein, IKAP, in mouse brains from different genotypes. Lane 1, positive control of nuclear extracts from HeLa cells, which are positive for IKAP expression; lane 2, control mouse (no human *IKBKAP* [WT] transgene); lane 3, *Ikbkap*$^{+/+}$ mouse with human WT transgene; lane 4, *Ikbkap*$^{-/-}$ mouse with human WT transgene; lane 5, *Ikbkap*$^{-/-}$ mouse with human FD transgene. Arrowhead 150-kDa position.

DISCUSSION

The identification of mutations in the *IKBKAP* gene in FD patients was a critical first step in the endeavor to find a treatment for FD (4, 7, 41). As a result of this discovery, it became clear that cellular levels of IKAP are diminished in a tissue-specific manner due to the IVS20+6T>C mutation, with the lowest levels observed in the nervous system. Even though the defective gene is now known, it is still unclear how reduction of IKAP during development leads to the observed neuropathy in FD. In order to begin to understand the role of IKAP in mammals, we created an *Ikbkap* knockout mouse model.

We demonstrated that *Ikbkap* expression is essential for embryonic development, as evidenced by embryonic lethality in the *Ikbkap*$^{-/-}$ embryos. Examination of embryos suggested that IKAP plays a crucial role in neuronal development. Expression of mouse Ikap can be detected in embryos at the early embryonic stage (8.5 dpc), with high expression in the primitive brain regions, notably the hindbrain, at the commencement of neurogenesis. At later embryonic stages (11.5 dpc), Ikap is expressed predominately in the dorsal root ganglia beside the spinal cord and in the roof plate area, where the progenitors of the cerebellum are born. Similar dorsal root ganglion expression has been reported previously in rat embryo studies using in situ hybridization (34). These unique expression patterns in the developing central and peripheral nervous system are consistent with the disoriented neural tube and absence of a primitive brain in the *Ikbkap*$^{-/-}$ embryos.

In this study, we demonstrated for the first time a role for *Ikbkap* in the proper development of the extraembryonic components of the conceptus, including the placenta and yolk sac. The visceral yolk sac functions as the metabolic center for the embryo during early development (3, 15). The yolk sac not only acts as a protective barrier for the embryo against the external environment, it is also involved in the transmission of nutrition from the uterus, as well as the disposal of toxins from the embryo prior to the development of the placenta and fetal liver. In addition, several molecules that are important for tissue remodeling, such as tissue plasminogen activator, as well as proteinases and inhibitors, are secreted by the visceral yolk sac (26). Over the past decade, with the advance of gene-targeting technology, several genes, such as *Vegfa* (6), *Flt1* (16), *Tgfb1* (14), *Angpt1* (45), *Tie1*/*Tie2* (37, 40), *Gata6* (27), and *Hnf4a* (9), have been shown to be crucial for visceral yolk sac development. The abnormalities observed in the *Ikbkap*$^{-/-}$ visceral yolk sac during gastrulation, such as the delayed onset of blood island formation and failure of blood vessel development, in part have similarities to the knockout phenotypes of these genes, suggesting that vasculogenesis and angiogenesis are impaired in the absence of *Ikbkap*. In the *Ikbkap*$^{-/-}$ visceral yolk sac, the formation of the primitive capillary plexus at 9.5 dpc, in conjunction with the absence of subsequent events, such as the establishment and increased thickness of the lumen and neovascularization, indicates that vasculogenesis was initiated but the subsequent angiogenesis was disrupted. Despite our demonstration of gene expression changes, further studies will be required to determine the precise role of *Ikbkap* in this vital developmental process.

Although the abnormalities of the *Ikbkap*$^{-/-}$ yolk sac exhibit similarities to some other gene-targeting studies that led to embryonic lethality, the developmental deficits observed in the *Ikbkap*$^{-/-}$ embryos are unique. In the *Tgfb1* knockout mouse model, the authors demonstrated that 50% of the *TGFb1*$^{-/-}$ and 25% of the *TGFb1*$^{+/-}$ embryos were prenatal lethal around 10.5 dpc as a result of the failure of the vascular and hematopoietic system functions and not due to direct effects on the nervous system in null embryos (14). In contrast, the *Ikbkap*$^{-/-}$ embryo exhibited a more dramatic phenotype; no *Ikbkap*$^{-/-}$ embryos were recovered beyond 12.5 dpc and severe neurodevelopmental defects were observed at earlier stages. Interestingly, at 9.5 dpc, the *Ikbkap*$^{-/-}$ embryo exhibits the classic features of gastrulation, such as open head fold, allantois, and primitive vascular organization, which normally occur in the wild-type embryos at 7.5 dpc, suggesting that *Ikbkap* might be involved in the signaling cascade that controls the transition from the primitive streak stage to gastrulation, such as proliferation and/or differentiation of progenitor cells. The fact that the anterior-posterior polarity of the *Ikbkap*$^{-/-}$ embryos was established eventually, as evidenced by the head-tail appearance at 9.5 dpc, suggests that *Ikbkap* might be involved in modulating this event via transcriptional regulation.

Examination of the embryos suggested that death occurred at 10.5 dpc. In fact the *Ikbkap*$^{-/-}$ embryos at 10 dpc appeared to be larger than those at 9.5 dpc, suggesting that the embryos lacking *Ikbkap* continue to develop during this period. Further,

at 10.5 dpc, the anterior neural tube was found to be closed, although the structure was distinct from that observed in the *Ikbkap*$^{+/+}$ embryos. In addition, the demonstration of disoriented alignment of the posterior neural tube in the *Ikbkap*$^{-/-}$ embryos reinforces the argument that neural-plate morphogenesis is still ongoing between 9.5 and 10.5 dpc. The irregularity of the neural-tube architecture, as well as the reduced expression of *Bmp4* and *Rhoa*, both of which are important for roof plate patterning in vertebrates, suggests that neurulation is disrupted in the absence of *Ikbkap* (31, 32, 48). Interestingly, ablating *Bmp4* not only led to embryonic lethality during gastrulation, but some of the *Bmp4* null embryos showed open head folds and an unturned body (49), similar to what was observed in the *Ikbkap*$^{-/-}$ embryos at the corresponding stage. However, the *Bmp4* null embryos did not advance to the postgastrulation stage as seen in the *Ikbkap*$^{-/-}$ embryos, and the size of the *Bmp4* null embryos was similar to that of controls while the overall size of the *Ikbkap*$^{-/-}$ embryo was dramatically reduced. In the future, it would be interesting to investigate the interaction between *Ikbkap* and BMP signaling, given the observed reduction of *Bmp4* expression in *Ikbkap*$^{-/-}$ embryos. In the *Ikbkap*$^{-/-}$ embryos, the level of *Ctnnb1*, a gene that is particularly important for brain formation and craniofacial development (5), was reduced. The function of *Ctnnb1* during gastrulation has been demonstrated by the embryonic lethality resulting from the failure in the formation of ectodermal cell layers in the *Ctnnb1* null embryo (18). The fact that the *Ctnnb1*$^{-/-}$ embryo cannot develop beyond gastrulation, unlike the *Ikbkap*$^{-/-}$ embryos, raises the possibility that in the absence of *Ikbkap*, another unknown signaling pathway might be compensating for the defect of *Ctnnb1* signaling, or more likely, expression of this gene might not be totally abolished in the *Ikbkap*$^{-/-}$ embryos. Taken together, our findings suggest that *Ikbkap*$^{-/-}$ embryos undergo early development and advance to the late gastrulation stage in an environment without *Ikbkap*. However, the disturbances in both vascular and neural development lead to lethality immediately following gastrulation.

Recently, several genes that require IKAP/Elongator have been identified by using either FD fibroblasts or HeLa cells in which RNA interference was used to reduce *IKBKAP* expression (8, 10). Further, RNA microarray studies using postmortem FD tissue suggest that a subset of genes involved in myelination might require IKAP for efficient transcription (8). In the current study, we tested the expression pattern of a subset of these genes in *Ikbkap*$^{-/-}$ embryos and did not find any reduction in expression. However, we did find reduced or absent expression of several genes required for embryogenesis. Our ChIP analysis of these genes demonstrated that in the absence of IKAP, histone H3 acetylation is significantly reduced in the 3′ ends of genes, although similar levels are observed close to the promoter. This is similar to the patterns observed in the FD fibroblasts and supports the previously described model for Elongator function as a histone acetyltransferase involved in transcriptional elongation (10). It is interesting that different Elongator dependences for the expression of individual genes are observed in the in vitro knockdown and in vivo knockout systems. This might be attributed to different gene expression patterns, or perhaps to changes in local chromatin structure, during development. These results may also suggest that specific genes have either developmental or tissue-specific thresholds for their reliance on IKAP/Elongator. Finally, the observed variability in Elongator dependence illustrates the complicated cascade of transcriptional regulation and the difficulty in assessing direct targets in tissues based on effects observed in cells in culture.

In conclusion, we have shown for the first time that IKAP is required for embryogenesis in mammals. Although the precise cause of embryonic lethality remains to be determined, our findings indicate that IKAP is required for entry from the egg cylinder stage into the gastrulation stage, as well as for proper neurulation and primitive organ development. Further, the function of IKAP is not restricted to the embryo, since striking abnormalities were also seen in the visceral yolk sac. Our work further demonstrating rescue of embryonic lethality by a human *IKBKAP* transgene is exciting, as it suggests functional conservation between the mouse and human proteins. Despite the fact that low levels of normal IKAP are expressed from the human transgene carrying the FD splicing mutation, the transgene does not rescue lethality. It does, however, suggest that increasing IKAP expression from the FD transgene using the small molecule kinetin (22) may enable us to achieve our ultimate goal of creating a phenotypically accurate mouse model of FD.

ACKNOWLEDGMENTS

We thank Felicia Axelrod and Gabrielle Gold von Simson of the Dysautonomia Treatment and Evaluation Center at New York University Medical School for their longstanding collaboration and helpful discussions. We thank James Gusella and Marcy MacDonald for their helpful discussions when we initiated this project and Jesper Svejstrup and Pierre Close for their advice on the ChIP studies.

This work was supported by grants from the Dysautonomia Foundation, Inc., and the National Institute for Neurological Disorders and Stroke.

REFERENCES

1. **Anderson, S. L., R. Coli, I. W. Daly, E. A. Kichula, M. J. Rork, S. A. Volpi, J. Ekstein, and B. Y. Rubin.** 2001. Familial dysautonomia is caused by mutations of the IKAP gene. Am. J. Hum. Genet. **68:**753–758.
2. **Axelrod, F. B.** 1995. Familial dysautonomia, p. 217–231. *In* D. Robertson and I. Biaggioni (ed.), Disorders of the autonomic nervous system. Harwood Academic Publishers, Luxembourg.
3. **Baron, M. H.** 2003. Embryonic origins of mammalian hematopoiesis. Exp. Hematol. **31:**1160–1169.
4. **Blumenfeld, A., S. A. Slaugenhaupt, C. B. Liebert, V. Temper, C. Maayan, S. Gill, D. E. Lucente, M. Idelson, K. MacCormack, M. A. Monahan, J. Mull, M. Leyne, M. Mendillo, T. Schiripo, E. Mishori, X. Breakefield, F. B. Axelrod, and J. F. Gusella.** 1999. Precise genetic mapping and haplotype analysis of the familial dysautonomia gene on human chromosome 9q31. Am. J. Hum. Genet. **64:**1110–1118.
5. **Brault, V., R. Moore, S. Kutsch, M. Ishibashi, D. H. Rowitch, A. P. McMahon, L. Sommer, O. Boussadia, and R. Kemler.** 2001. Inactivation of the beta-catenin gene by Wnt1-Cre-mediated deletion results in dramatic brain malformation and failure of craniofacial development. Development **128:**1253–1264.
6. **Carmeliet, P., V. Ferreira, G. Breier, S. Pollefeyt, L. Kieckens, M. Gertsenstein, M. Fahrig, A. Vandenhoeck, K. Harpal, C. Eberhardt, C. Declercq, J. Pawling, L. Moons, D. Collen, W. Risau, and A. Nagy.** 1996. Abnormal blood vessel development and lethality in embryos lacking a single VEGF allele. Nature **380:**435–439.
7. **Chadwick, B. P., S. Gill, M. Leyne, J. Mull, C. B. Liebert, C. M. Robbins, H. W. Pinkett, I. Makalowska, C. Maayan, A. Blumenfeld, F. B. Axelrod, M. Brownstein, and S. A. Slaugenhaupt.** 1999. Cloning, genomic organization and expression of a putative human transmembrane protein related to the *Caenorhabditis elegans* M01F1.4 gene. Gene **240:**67–73.
8. **Cheishvili, D., C. Maayan, Y. Smith, G. Ast, and A. Razin.** 2007. IKAP/hELP1 deficiency in the cerebrum of familial dysautonomia patients results in down regulation of genes involved in oligodendrocyte differentiation and in myelination. Hum. Mol. Genet. **16:**2097–2104.

9. **Chen, W. S., K. Manova, D. C. Weinstein, S. A. Duncan, A. S. Plump, V. R. Prezioso, R. F. Bachvarova, and J. E. Darnell, Jr.** 1994. Disruption of the HNF-4 gene, expressed in visceral endoderm, leads to cell death in embryonic ectoderm and impaired gastrulation of mouse embryos. Genes Dev. **8:**2466–2477.
10. **Close, P., N. Hawkes, I. Cornez, C. Creppe, C. A. Lambert, B. Rogister, U. Siebenlist, M. P. Merville, S. A. Slaugenhaupt, V. Bours, J. Q. Svejstrup, and A. Chariot.** 2006. Transcription impairment and cell migration defects in elongator-depleted cells: implication for familial dysautonomia. Mol. Cell **22:**521–531.
11. **Cohen, L., W. J. Henzel, and P. A. Baeuerle.** 1998. IKAP is a scaffold protein of the IκB kinase complex. Nature **395:**292–296.
12. **Cuajungco, M. P., M. Leyne, J. Mull, S. P. Gill, J. F. Gusella, and S. A. Slaugenhaupt.** 2001. Cloning, characterization, and genomic structure of the mouse Ikbkap gene. DNA Cell Biol. **20:**579–586.
13. **Cuajungco, M. P., M. Leyne, J. Mull, S. P. Gill, W. Lu, D. Zagzag, F. B. Axelrod, C. Maayan, J. F. Gusella, and S. A. Slaugenhaupt.** 2003. Tissue-specific reduction in splicing efficiency of IKBKAP due to the major mutation associated with familial dysautonomia. Am. J. Hum. Genet. **72:**749–758.
14. **Dickson, M. C., J. S. Martin, F. M. Cousins, A. B. Kulkarni, S. Karlsson, and R. J. Akhurst.** 1995. Defective haematopoiesis and vasculogenesis in transforming growth factor-beta 1 knock out mice. Development **121:**1845–1854.
15. **Dzierzak, E., and A. Medvinsky.** 1995. Mouse embryonic hematopoiesis. Trends Genet. **11:**359–366.
16. **Fong, G. H., J. Rossant, M. Gertsenstein, and M. L. Breitman.** 1995. Role of the Flt-1 receptor tyrosine kinase in regulating the assembly of vascular endothelium. Nature **376:**66–70.
17. **Gold-von Simson, G., and F. B. Axelrod.** 2006. Familial dysautonomia: update and recent advances. Curr. Probl. Pediatr. Adolesc. Health Care **36:** 218–237.
18. **Haegel, H., L. Larue, M. Ohsugi, L. Fedorov, K. Herrenknecht, and R. Kemler.** 1995. Lack of beta-catenin affects mouse development at gastrulation. Development **121:**3529–3537.
19. **Hawkes, N. A., G. Otero, G. S. Winkler, N. Marshall, M. E. Dahmus, D. Krappmann, C. Scheidereit, C. L. Thomas, G. Schiavo, H. Erdjument-Bromage, P. Tempst, and J. Q. Svejstrup.** 2002. Purification and characterization of the human elongator complex. J. Biol. Chem. **277:**3047–3052.
20. **Hebbes, T. R., A. W. Thorne, and C. Crane-Robinson.** 1988. A direct link between core histone acetylation and transcriptionally active chromatin. EMBO J. **7:**1395–1402.
21. **Hilz, M. J., E. H. Kolodny, I. Neuner, B. Stemper, and F. B. Axelrod.** 1998. Highly abnormal thermotests in familial dysautonomia suggest increased cardiac autonomic risk. J. Neurol. Neurosurg. Psychiatry **65:**338–343.
22. **Hims, M. M., C. el Ibrahim, M. Leyne, J. Mull, L. Liu, C. Lazaro, R. S. Shetty, S. Gill, J. F. Gusella, R. Reed, and S. A. Slaugenhaupt.** 2007. Therapeutic potential and mechanism of kinetin as a treatment for the human splicing disease familial dysautonomia. J. Mol. Med. **85:**149–161.
23. **Hims, M. M., R. S. Shetty, J. Pickel, J. Mull, M. Leyne, L. Liu, J. F. Gusella, and S. A. Slaugenhaupt.** 2007. A humanized IKBKAP transgenic mouse models a tissue-specific human splicing defect. Genomics **90:**389–396.
24. **Holmberg, C., S. Katz, M. Lerdrup, T. Herdegen, M. Jaattela, A. Aronheim, and T. Kallunki.** 2002. A novel specific role for I kappa B kinase complex-associated protein in cytosolic stress signaling. J. Biol. Chem. **277:**31918–31928.
25. **Jablonowski, D., S. Zink, C. Mehlgarten, G. Daum, and R. Schaffrath.** 2006. tRNAGlu wobble uridine methylation by Trm9 identifies Elongator's key role for zymocin-induced cell death in yeast. Mol. Microbiol. **59:**677–688.
26. **Jones, C. J., and E. Jauniaux.** 1995. Ultrastructure of the materno-embryonic interface in the first trimester of pregnancy. Micron **26:**145–173.
27. **Koutsourakis, M., A. Langeveld, R. Patient, R. Beddington, and F. Grosveld.** 1999. The transcription factor GATA6 is essential for early extraembryonic development. Development **126:**723–732.
28. **Krappmann, D., E. N. Hatada, S. Tegethoff, J. Li, A. Klippel, K. Giese, P. A. Baeuerle, and C. Scheidereit.** 2000. The I kappa B kinase (IKK) complex is tripartite and contains IKK gamma but not IKAP as a regular component. J. Biol. Chem. **275:**29779–29787.
29. **Lehavi, O., O. Aizenstein, D. Bercovich, D. Pavzner, R. Shomrat, A. Orr-Urtreger, and Y. Yaron.** 2003. Screening for familial dysautonomia in Israel: evidence for higher carrier rate among Polish Ashkenazi Jews. Genet. Test. **7:**139–142.
30. **Leyne, M., J. Mull, S. P. Gill, M. P. Cuajungco, C. Oddoux, A. Blumenfeld, C. Maayan, J. F. Gusella, F. B. Axelrod, and S. A. Slaugenhaupt.** 2003. Identification of the first non-Jewish mutation in familial dysautonomia. Am. J. Med. Genet. A **118:**305–308.
31. **Liem, K. F., Jr., G. Tremml, and T. M. Jessell.** 1997. A role for the roof plate and its resident TGFβ-related proteins in neuronal patterning in the dorsal spinal cord. Cell **91:**127–138.
32. **Liu, A., and L. A. Niswander.** 2005. Bone morphogenetic protein signalling and vertebrate nervous system development. Nat. Rev. Neurosci. **6:**945–954.
33. **Maayan, C., E. Kaplan, S. Shachar, O. Peleg, and S. Godfrey.** 1987. Incidence of familial dysautonomia in Israel 1977–1981. Clin. Genet. **32:**106–108.
34. **Mezey, E., A. Parmalee, I. Szalayova, S. P. Gill, M. P. Cuajungco, M. Leyne, S. A. Slaugenhaupt, and M. J. Brownstein.** 2003. Of splice and men: what does the distribution of IKAP mRNA in the rat tell us about the pathogenesis of familial dysautonomia? Brain Res. **983:**209–214.
35. **Nord, A. S., P. J. Chang, B. R. Conklin, A. V. Cox, C. A. Harper, G. G. Hicks, C. C. Huang, S. J. Johns, M. Kawamoto, S. Liu, E. C. Meng, J. H. Morris, J. Rossant, P. Ruiz, W. C. Skarnes, P. Soriano, W. L. Stanford, D. Stryke, H. von Melchner, W. Wurst, K. Yamamura, S. G. Young, P. C. Babbitt, and T. E. Ferrin.** 2006. The International Gene Trap Consortium website: a portal to all publicly available gene trap cell lines in mouse. Nucleic Acids Res. **34:**D642–D648.
36. **Otero, G., J. Fellows, Y. Li, T. de Bizemont, A. M. Dirac, C. M. Gustafsson, H. Erdjument-Bromage, P. Tempst, and J. Q. Svejstrup.** 1999. Elongator, a multisubunit component of a novel RNA polymerase II holoenzyme for transcriptional elongation. Mol. Cell **3:**109–118.
37. **Patan, S.** 1998. TIE1 and TIE2 receptor tyrosine kinases inversely regulate embryonic angiogenesis by the mechanism of intussusceptive microvascular growth. Microvasc. Res. **56:**1–21.
38. **Pearson, J.** 1979. Familial dysautonomia (a brief review). J. Auton. Nerv Syst. **1:**119–126.
39. **Rahl, P. B., C. Z. Chen, and R. N. Collins.** 2005. Elp1p, the yeast homolog of the FD disease syndrome protein, negatively regulates exocytosis independently of transcriptional elongation. Mol. Cell **17:**841–853.
40. **Sato, T. N., Y. Tozawa, U. Deutsch, K. Wolburg-Buchholz, Y. Fujiwara, M. Gendron-Maguire, T. Gridley, H. Wolburg, W. Risau, and Y. Qin.** 1995. Distinct roles of the receptor tyrosine kinases Tie-1 and Tie-2 in blood vessel formation. Nature **376:**70–74.
41. **Slaugenhaupt, S. A., A. Blumenfeld, S. P. Gill, M. Leyne, J. Mull, M. P. Cuajungco, C. B. Liebert, B. Chadwick, M. Idelson, L. Reznik, C. Robbins, I. Makalowska, M. Brownstein, D. Krappmann, C. Scheidereit, C. Maayan, F. B. Axelrod, and J. F. Gusella.** 2001. Tissue-specific expression of a splicing mutation in the IKBKAP gene causes familial dysautonomia. Am. J. Hum. Genet. **68:**598–605.
42. **Slaugenhaupt, S. A., and J. F. Gusella.** 2002. Familial dysautonomia. Curr. Opin. Genet. Dev. **12:**307–311.
43. **Stanford, W. L., T. Epp, T. Reid, and J. Rossant.** 2006. Gene trapping in embryonic stem cells. Methods Enzymol. **420:**136–162.
44. **Struhl, K.** 1998. Histone acetylation and transcriptional regulatory mechanisms. Genes Dev. **12:**599–606.
45. **Suri, C., P. F. Jones, S. Patan, S. Bartunkova, P. C. Maisonpierre, S. Davis, T. N. Sato, and G. D. Yancopoulos.** 1996. Requisite role of angiopoietin-1, a ligand for the TIE2 receptor, during embryonic angiogenesis. Cell **87:**1171–1180.
46. **Svejstrup, J. Q.** 2007. Elongator complex: how many roles does it play? Curr. Opin. Cell Biol. **19:**331–336.
47. **Waldrip, W. R., E. K. Bikoff, P. A. Hoodless, J. L. Wrana, and E. J. Robertson.** 1998. Smad2 signaling in extraembryonic tissues determines anterior-posterior polarity of the early mouse embryo. Cell **92:**797–808.
48. **Wallingford, J. B., and R. M. Harland.** 2002. Neural tube closure requires Dishevelled-dependent convergent extension of the midline. Development **129:**5815–5825.
49. **Winnier, G., M. Blessing, P. A. Labosky, and B. L. Hogan.** 1995. Bone morphogenetic protein-4 is required for mesoderm formation and patterning in the mouse. Genes Dev. **9:**2105–2116.